

M. Destrade
M. D. Gilchrist

School of Electrical, Electronic, and Mechanical
Engineering,
University College Dublin,
Belfield,
Dublin 4, Ireland

D. A. Prikazchikov

Department of Advanced and Applied
Mathematics,
The Russian State Open Technical University of
Railway Transport,
Chasovaya Street,
Moscow 22/2, Russia

G. Saccomandi

Dipartimento di Ingegneria Industriale,
Università degli Studi di Perugia,
06125 Perugia, Italy

Surface Instability of Sheared Soft Tissues

When a block made of an elastomer is subjected to a large shear, its surface remains flat. When a block of biological soft tissue is subjected to a large shear, it is likely that its surface in the plane of shear will buckle (appearance of wrinkles). One factor that distinguishes soft tissues from rubberlike solids is the presence—sometimes visible to the naked eye—of oriented collagen fiber bundles, which are stiffer than the elastin matrix into which they are embedded but are nonetheless flexible and extensible. Here we show that the simplest model of isotropic nonlinear elasticity, namely, the incompressible neo-Hookean model, suffers surface instability in shear only at tremendous amounts of shear, i.e., above 3.09, which corresponds to a 72 deg angle of shear. Next we incorporate a family of parallel fibers in the model and show that the resulting solid can be either reinforced or strongly weakened with respect to surface instability, depending on the angle between the fibers and the direction of shear and depending on the ratio E/μ between the stiffness of the fibers and that of the matrix. For this ratio we use values compatible with experimental data on soft tissues. Broadly speaking, we find that the surface becomes rapidly unstable when the shear takes place “against” the fibers and that as E/μ increases, so does the sector of angles where early instability is expected to occur. [DOI: 10.1115/1.2979869]

Keywords: soft tissues, large shear, extensible fibers, mechanical instability

1 Introduction

Rubberlike solids and biological soft tissues can both be efficiently modeled within the framework of finite elasticity, which can account for large deformations, physical nonlinearities, incompressibility, residual stresses, viscoelasticity, etc. One of the most salient differences between the two types of solids is that at rest, elastomers are essentially isotropic while soft tissues are essentially anisotropic because of the presence of collagen fiber bundles. In that respect, it is worthwhile to consider the effect of incorporating families of parallel fibers into an isotropic matrix and see if it can model some striking differences between the mechanical behavior of elastomers and that of soft tissues. Consider, for instance, the large shear of a solid block. When the block is made of an elastomer such as silicone, its surface remains stable; when it is made of a biological soft tissue such as a skeletal muscle, its surface wrinkles for certain ranges of orientation between the direction of shear and the (presumed) direction of fibers (see Fig. 1). Here we show that one of the simplest models of anisotropic nonlinear elasticity, which requires only knowledge of the fiber/matrix stiffness ratio, is sufficient to successfully predict these behaviors.

To model the isotropic elastomer (Sec. 2), we take the incompressible neo-Hookean solid and find that it does not suffer surface instability unless it is subjected to a substantial amount of shear (critical amount of shear: 3.09; critical angle of shear: 72 deg). In that case the wrinkles are aligned with the direction of greatest stretch. (The wrinkling analysis relies on the incremental theory of nonlinear elasticity; see, for instance, Biot [1] or Ogden [2]). Next, we introduce one family of parallel fibers into the model (Sec. 3). To model biological soft tissues with one preferred direction (Sec. 4), we take the incompressible neo-Hookean strain energy density, augmented by the so-called “standard rein-

forcing model”: this model has only two parameters, namely, the shear modulus μ of the soft (neo-Hookean) matrix and the fiber stiffness E .

With respect to surface instability, only the ratio E/μ of these two quantities plays a role. We take it to be equal, in turn, to 40.0, 20.0, and 10.0, in agreement with the range of experimental measures found in the literature. We then find that when the angle between the direction of shear and the direction of the fibers is small, the solid is much more stable than the isotropic solid obtained in the absence of fibers; when the angle increases but is less than 99.0 deg (for $E/\mu=40.0$), 102.8 deg (for $E/\mu=20.0$), and 108.1 deg (for $E/\mu=10.0$), the solid remains more stable than the isotropic solid; however, when the angle exceeds those values, the critical amount of shear for surface instability drops to extremely low levels, indicating the appearance of wrinkles as soon as shearing occurs. In that case, the wrinkles are found to be almost orthogonal to the fibers, in accordance with visual observations.

It is hoped that the paper provides a greater understanding of the causes of certain instabilities in soft tissues and a quantitative tool to measure what deformations (critical amounts of shear) are permissible and in which directions. Surface instability has a direct connection to slab and tube buckling, which in biomechanics may potentially translate into aneurysm formation, arterial kinking and tortuosity, brain trauma, and many other, still not well understood, pathologies.

2 Surface Instability of a Sheared Isotropic Solid

First, we recall known results in the theory of surface wrinkling valid for *isotropic* solids.

Consider a semi-infinite body made of an incompressible isotropic neo-Hookean solid, for which the strain energy function W , written as a function of the principal stretch ratios λ_1 , λ_2 , and λ_3 , is given by

$$W = \mu(\lambda_1^2 + \lambda_2^2 + \lambda_3^2 - 3)/2 \quad (1)$$

Here μ is the shear modulus, and $\lambda_1\lambda_2\lambda_3=1$ by the incompressibility constraint. Then subject the solid to a large homogeneous static deformation, such that λ_2 is the stretch ratio along the normal to the free surface. It has long been known that the surface

Contributed by the Bioengineering Division of ASME for publication in the JOURNAL OF BIOMECHANICAL ENGINEERING. Manuscript received March 13, 2008; final manuscript received April 22, 2008; published online October 10, 2008. Review conducted by Ellen M. Arruda.

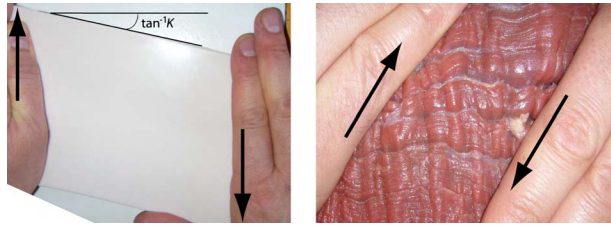


Fig. 1 Shearing (along the arrows) a block of silicone of approximate size $15 \times 10 \times 1.5 \text{ cm}^3$ and a block of mammalian skeletal muscle (beef) of approximate size $15 \times 10 \times 3 \text{ cm}^3$. One does not exhibit surface instability, the other does.

becomes unstable when the following *wrinkling condition* is met:

$$\lambda_1^2 \lambda_3 = \sigma_0 \quad (2)$$

where $\sigma_0 \approx 0.296$ is the real root of $\sigma^3 + \sigma^2 + 3\sigma - 1 = 0$ (Green and Zerna [3]; Biot [1]).

In the following *plane strain* situation:

$$\lambda_1 = \lambda, \quad \lambda_2 = 1, \quad \lambda_3 = \lambda^{-1} \quad (3)$$

the critical stretch of compression found from Eq. (2) is clearly $\lambda_1 = \sigma_0 \approx 0.296$ (and then $\lambda_3 = \sigma_0^{-1} \approx 3.38$). The conclusion is that when a semi-infinite neo-Hookean solid, which is neither allowed to expand nor contract along the normal to its boundary, is *compressed* by 71% in a given direction (lying in the boundary), it buckles with wrinkles developing along the direction *orthogonal* to the direction of compression. Equivalently, when it is *stretched* by 238%, it buckles with wrinkles *parallel* to the direction of tension. Figure 2 summarizes these results.

It is natural to wonder whether the surface might have become unstable in other directions earlier, that is, at compressive (≤ 1) ratios larger than 0.296 or at tensile (≥ 1) ratios smaller than 3.38. Flavin [4] showed that wrinkles develop parallel to the direction, making an angle θ with the principal direction of strain associated with the stretch ratio λ_3 when the following wrinkling condition is met:

$$\lambda_1^2 \lambda_3^2 (\lambda_1^2 \cos^2 \theta + \lambda_3^2 \sin^2 \theta) = \sigma_0^2 \quad (4)$$

In the plane strain situation (Eq. (3)), this condition is quadratic in λ^2 ,

$$\lambda^4 \cos^2 \theta - \lambda^2 \sigma_0^2 + \sin^2 \theta = 0 \quad (5)$$

It has real roots provided that θ is in the range $-\theta_0 \leq \theta \leq \theta_0$ or $\pi/2 - \theta_0 \leq \theta \leq \pi/2 + \theta_0$, where $\theta_0 = (1/2) \sin^{-1} \sigma_0^2 \approx 2.51$ deg. In the former range, the compressive critical stretch found from the biquadratic equation (Eq. (5)) turns out to be smaller than 0.296 and, in the latter range, to be larger than 3.38. Thus surface instability for the plane strain equation (Eq. (3)) occurs when the isotropic neo-Hookean half-space is in compression at a ratio σ_0 or, equivalently, in tension at a ratio σ_0^{-1} . The *wrinkles are parallel to the direction of greatest stretch* and orthogonal to the direction of greatest compression.

Now *simple shear* belongs to the family of plane strains (Eq. (3)), with the following connection between the principal stretches and the amount of shear K (see Ogden [2], for instance):

$$K = \lambda - \lambda^{-1}, \quad \lambda = K/2 + \sqrt{1 + K^2/4} \quad (6)$$

Also, the direction of greatest stretch is at an angle ψ with the direction of shear, where $\psi \in]0, \pi/4]$ is given by

$$\tan 2\psi = 2/K \quad (7)$$

Clearly $\lambda > 1$ here, and so surface shear instability occurs in tension when the amount of shear is equal to $K_0 = \sigma_0^{-1} - \sigma_0 \approx 3.09$. The corresponding critical angle of shear is then $\tan^{-1} K_0 \approx 72.0$ deg (see Fig. 3). This is a quite large shear.

3 Sheared Fiber-Reinforced Solids

3.1 Finite Simple Shear. Now we consider a semi-infinite composite incompressible solid made of an isotropic matrix reinforced with one family of parallel extensible fibers, themselves parallel to the boundary of the solid. In the undeformed configuration, we call (X_1, X_2, X_3) the set of Cartesian coordinates such

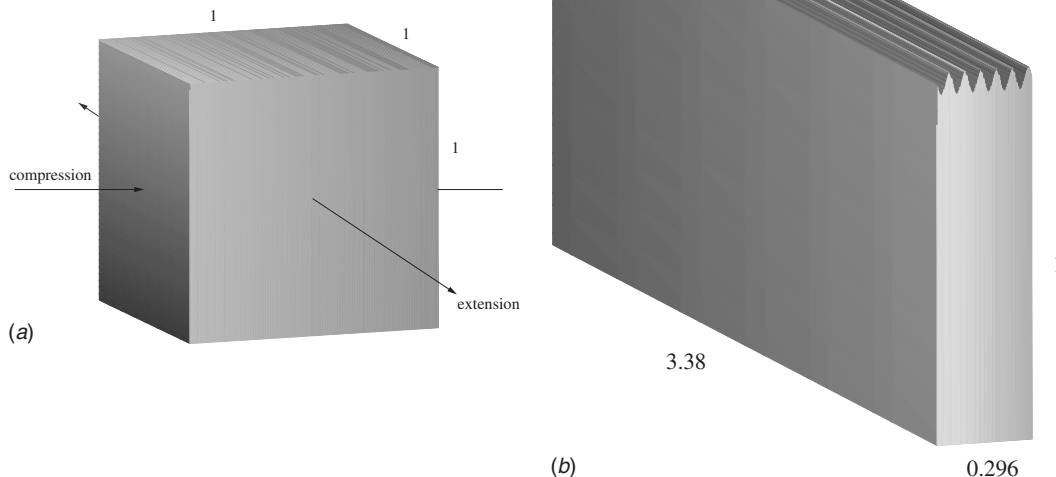


Fig. 2 Large plane strain deformation of a unit cube near the surface of a semi-infinite incompressible neo-Hookean solid. When the solid is compressed by 71% (or, equivalently, stretched by 238%), its surface wrinkles. Note that the analysis quantifies neither the amplitude nor the wavelength of the wrinkles.

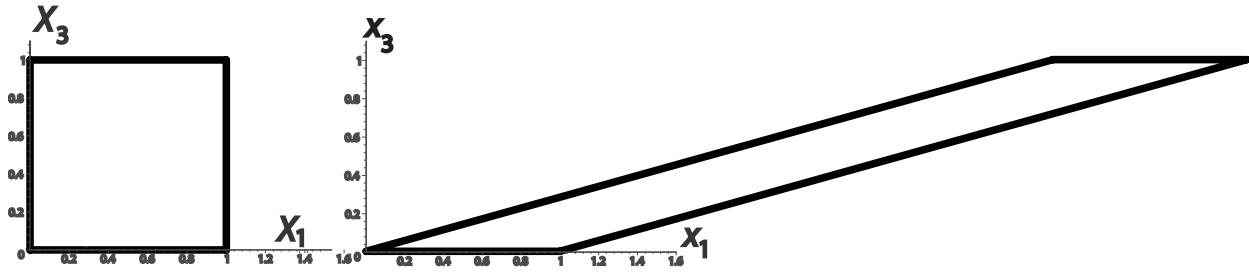


Fig. 3 Large simple shear of a unit square in the surface of a semi-infinite incompressible neo-Hookean solid. When the solid is sheared by an amount $K_0 \approx 3.09$ (figure on the right), its surface wrinkles. The corresponding angle of shear is $\tan^{-1} K_0 \approx 72.0$ deg, which is physically abnormally large. Then the wrinkles are parallel to the direction of greatest tension, which makes an angle $\varphi_0 \approx 16.5$ deg with the direction of shear (and so, the wrinkles are almost aligned with the sheared faces).

that the solid is located in the $X_2 \geq 0$ region. We denote by $E_1, E_2,$ and E_3 the orthogonal unit vectors defining the Lagrangian (reference) axes, aligned with the $X_1, X_2,$ and X_3 directions, respectively.

When the solid is sheared in the direction of E_1 , the particle at X moves to its current position x . We call $F = \partial x / \partial X$ the associated deformation gradient tensor and $B = FF^T$ the left Cauchy–Green strain tensor. We then call (x_1, x_2, x_3) the Cartesian coordinates, aligned with (X_1, X_2, X_3) , corresponding to the current position x . In the current configuration, the basis vectors are $e_1, e_2,$ and e_3 , and here they are such that $e_i \equiv E_i$ ($i=1,2,3$). The simple shear of amount K is described by

$$x_1 = X_1 + KX_3, \quad x_2 = X_2, \quad x_3 = X_3 \quad (8)$$

We thus find, in turn, that

$$F = I + Ke_1 \otimes E_3, \quad B = I + K(e_1 \otimes e_3 + e_1 \otimes e_3) + K^2 e_1 \otimes e_1 \quad (9)$$

The principal stretches are given by Eqs. (3) and (6), and the first principal isotropic invariant $I_1 = \text{tr} B$ is given here by

$$I_1 = 3 + K^2 \quad (10)$$

Note that for shear, the second principal isotropic invariant, $I_2 = [I_1^2 - \text{tr}(B^2)]/2$ is also equal to $3 + K^2$.

3.2 One Family of Fibers. For solids reinforced with one family of parallel fibers lying in the plane of shear, we work in all generality and consider that the angle Φ (say) between the fibers

and the X_1 direction can take any value. In other words, the unit vector M (say) in the preferred fiber direction has components

$$M = \cos \Phi E_1 + \sin \Phi E_3 \quad (11)$$

in the reference configuration. Simple shear is a homogeneous deformation, and so M is transformed into $m = FM$ in the current configuration, that is,

$$m = (\cos \Phi + K \sin \Phi) e_1 + \sin \Phi e_3 \quad (12)$$

Without loss of generality, we take the ranges $K \geq 0$ and $0 \leq \Phi \leq \pi$, which cover all possible orientations of the fibers with respect to the direction of shear.

To fix the ideas, consider Fig. 4. There we shear the half-space by a finite amount $K=0.5$, in the direction making an angle $\Phi = 60$ deg with the fibers. Notice that a unit vector n making an angle θ with the direction of shear is also represented in the current configuration. This is the normal to the wrinkles' front; in the next section we look for surface wrinkles in all directions (the angle θ spans the interval $[0 \text{ deg}, 180 \text{ deg}]$), and we determine which is the smallest corresponding critical amount of shear.

Finally we introduce the anisotropic invariants $I_4 \equiv m \cdot m$ and $I_5 \equiv Fm \cdot Fm$; in particular, we find

$$I_4 = 1 + K \sin 2\Phi + K^2 \sin^2 \Phi \quad (13)$$

Recall that I_4 is the squared stretch in the fiber direction [5]. In particular, if $I_4 \geq 1$ then the fibers are in extension, and if $I_4 \leq 1$ then they are in compression. Clearly here, when $0 \leq \Phi \leq \pi/2$, the fibers are always in extension but when $\pi/2 < \Phi < \pi$, there exists

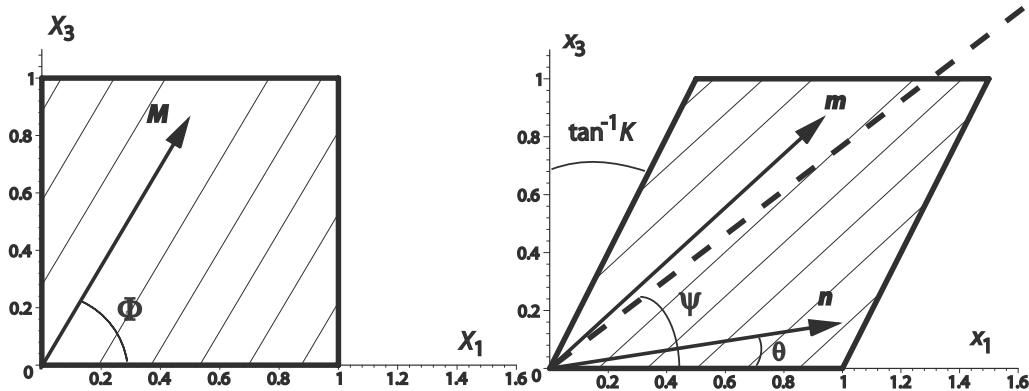


Fig. 4 A unit square lying on the surface of a semi-infinite solid reinforced with one family of fibers (thin lines) and subject to a simple shear of amount $K=0.5$ (the angle of shear is $\tan^{-1} K \approx 26.6$ deg) in the X_1 direction. In the reference configuration, the fibers are along the unit vector M at the angle $\Phi=60$ deg with the X_1 -axis. In the current configuration, they are along m . The unit vector n is orthogonal to the wrinkles' front (when they exist). Finally, the dashed line is aligned with the direction of greatest stretch; it is at an angle $\psi \approx 38$ deg to the direction of shear.

a certain amount of shear (explicitly, $-2/\tan \Phi$) below which the fibers are in compression.

3.3 Constitutive Assumptions. In general, the strain energy density W of a hyperelastic incompressible solid reinforced with one family of parallel extensible fibers depends on the isotropic invariants I_1 and I_2 and on the anisotropic invariants (Spencer [5]) I_4 and I_5 . We assume that W is the sum of an isotropic part and an anisotropic part. For the isotropic part, modeling the properties of the “soft” matrix, we take the neo-Hookean strain energy density in order to make a connection with the results of Sec. 2. For the anisotropic part, modeling the properties of the extensible “stiff” fibers, we take a function of I_4 only, say, $F(I_4)$. Hence, we restrict our attention to those solids with strain energy density,

$$W = \mu(I_1 - 3)/2 + F(I_4) \quad (14)$$

This assumption is quite common in the biomechanics literature. Although it does not prove crucial to the analysis, it leads to compact and revealing expressions. (Note that the consideration of a more general W poses no major extra difficulty but results in much longer expressions.)

The corresponding Cauchy stress tensor $\boldsymbol{\sigma}$ is (see, e.g., Ref. [6]): $\boldsymbol{\sigma} = -p\mathbf{I} + \mu\mathbf{B} + 2F'(I_4)\mathbf{m} \otimes \mathbf{m}$, where p is a Lagrange multiplier introduced by the constraint of incompressibility. The surface $x_2=0$ is free of tractions: here $\sigma_{12}=\sigma_{23}=0$ follows from $B_{12}=B_{23}=0$ and $\mathbf{m} \cdot \mathbf{e}_2=0$ (see Eqs. (9) and (12)), while $\sigma_{22}=0$ gives $p=\mu$. Thus, the prestress necessary to maintain the shear (Eq. (8)) is

$$\boldsymbol{\sigma} = \mu(\mathbf{B} - \mathbf{I}) + 2F'(I_4)\mathbf{m} \otimes \mathbf{m} \quad (15)$$

showing that the directions of principal stress and strain do not coincide in general (except when the preferred direction is aligned with principal directions of strain).

4 Surface Instability

4.1 Incremental Deformations. We seek solutions to the incremental equations of equilibrium and incremental boundary conditions in the form of sinusoidal perturbations whose amplitude decays rapidly with depth. In contrast to the isotropic case of Sec. 2, we do not know a priori in which direction the wrinkles should be aligned, and we take the normal to the wrinkles' front \mathbf{n} (say) to lie in the (x_1, x_3) plane at an arbitrary angle θ with x_1 (see Fig. 4). Hence, we seek a perturbation solution \mathbf{u} (mechanical displacement) and \dot{p} (increment of the Lagrange multiplier associated with incompressibility) in the form

$$\{\mathbf{u}, \dot{p}\} = \{\mathbf{U}(kx_2), ikP(kx_2)\}e^{ik(\cos \theta x_1 + \sin \theta x_3)} \quad (16)$$

where k is the “wave-number” and \mathbf{U} and P are functions of kx_2 alone.

The incremental equations read

$$s_{ji,j} = 0, \quad u_{j,j} = 0 \quad (17)$$

where the comma denotes partial differentiation with respect to x_j and s is the incremental nominal stress tensor. Its components are [2]

$$s_{ji} = \mathcal{A}_{0jilk}u_{k,l} + pu_{j,i} - \dot{p}\delta_{ij} \quad (18)$$

where \mathcal{A}_0 is the fourth-order tensor of instantaneous elastic moduli. In general it has a long expression for fiber-reinforced solids, with possibly 45 nonzero components (see, for example, Refs. [7,8]). For W in the form of Eq. (14), \mathbf{B} by Eq. (9), and \mathbf{M} by Eq. (11), we find the following components:

$$\mathcal{A}_{0jilk} = \mu\delta_{ik}B_{jl} + 2F'(I_4)\delta_{ik}m_j m_l + 4F''(I_4)m_i m_j m_k m_l \quad (19)$$

(see Merodio and Ogden [9]). Clearly, these components have the symmetries $\mathcal{A}_{0jilk} = \mathcal{A}_{0lkji}$ and $\mathcal{A}_{0jilk} = \mathcal{A}_{0jkli}$. We end up with 23 nonzero components, several of which are equal to one another (in

total there are 13 different components).

Clearly, if \mathbf{u} and \dot{p} are of the form of Eq. (16), then by Eq. (18) s_{ji} are of a similar form, say,

$$s_{ji} = ikS_{ji}(kx_2)e^{ik(\cos \theta x_1 + \sin \theta x_3)} \quad (20)$$

where S_{ji} are functions of the variable kx_2 only. By a systematic procedure, first laid down by Chadwick [10] (see also Refs. [11–14]), we can eliminate P and write the incremental equations of equilibrium as a first-order differential system. This is known as the *Stroh formulation* of the problem,

$$\begin{bmatrix} \mathbf{U}' \\ \mathbf{S}' \end{bmatrix} = iN \begin{bmatrix} \mathbf{U} \\ \mathbf{S} \end{bmatrix} \quad \text{where } \mathbf{U} = \begin{bmatrix} U_1 \\ U_2 \\ U_3 \end{bmatrix} \quad (21)$$

$$\mathbf{S} = \begin{bmatrix} S_{21} \\ S_{22} \\ S_{23} \end{bmatrix}, \quad N = \begin{bmatrix} N_1 & N_2 \\ N_3 & N_1 \end{bmatrix}$$

and the symmetric 3×3 matrices N_1 , N_2 , and N_3 are given by

$$-N_1 = \begin{bmatrix} 0 & \cos \theta & 0 \\ \cos \theta & 0 & \sin \theta \\ 0 & \sin \theta & 0 \end{bmatrix}, \quad N_2 = \begin{bmatrix} 1/\mu & 0 & 0 \\ 0 & 0 & 0 \\ 0 & 0 & 1/\mu \end{bmatrix} \quad (22)$$

$$-N_3 = \begin{bmatrix} \eta & 0 & \kappa \\ 0 & \nu & 0 \\ \kappa & 0 & \chi \end{bmatrix}$$

with

$$\eta = (\mathcal{A}_{01111} + 3\mu)\cos^2 \theta + 2\mathcal{A}_{01131}\cos \theta \sin \theta + \mathcal{A}_{03131}\sin^2 \theta$$

$$\nu = \mathcal{A}_{01212}\cos^2 \theta + 2\mathcal{A}_{01232}\cos \theta \sin \theta + \mathcal{A}_{03232}\sin^2 \theta - \mu$$

$$\chi = \mathcal{A}_{01313}\cos^2 \theta + 2\mathcal{A}_{01333}\cos \theta \sin \theta + (\mathcal{A}_{03333} + 3\mu)\sin^2 \theta$$

$$\kappa = \mathcal{A}_{01113}\cos^2 \theta + (2\mathcal{A}_{01133} + 3\mu)\cos \theta \sin \theta + \mathcal{A}_{03133}\sin^2 \theta \quad (23)$$

Notice how all the information relative to anisotropy is located in the N_3 matrix.

The solution to the system of Eq. (21) is clearly an exponential

$$\{\mathbf{U}, \mathbf{S}\} = \{\mathbf{U}^0, \mathbf{S}^0\}e^{ikqx_2} \quad (24)$$

where \mathbf{U}^0 and \mathbf{S}^0 are constant vectors and q is an eigenvalue of N . The characteristic equation associated with N is a *bicubic* [8],

$$q^6 - \left(2 - \frac{\chi + \eta}{\mu}\right)q^4 + \left(1 + \frac{\nu - 2\epsilon}{\mu} + \frac{\chi\eta - \kappa^2}{\mu^2}\right)q^2 + \frac{\epsilon(\mu + \nu)}{\mu^2} = 0 \quad (25)$$

where the quantity ϵ is defined by

$$\epsilon = \chi \cos^2 \theta - 2\kappa \cos \theta \sin \theta + \eta \sin^2 \theta \quad (26)$$

The existence of real roots in this equation corresponds to the loss of ellipticity of the governing equations (*material instabilities*). This possibility has been thoroughly investigated before (see Refs. [9,15,16]). Here we focus on complex roots and keep those satisfying $\text{Im } q > 0$ for a surface-type bifurcation, which decays with depth (*geometric instability*).

4.2 Wrinkling Condition and Resolution Scheme. Over the years, many schemes have been developed to solve surface boundary problems using the Stroh formulation; we used, in turn, the determinantal method [17], the Riccati matrix equation of surface impedance [13,14], and explicit polynomial equations [18] in

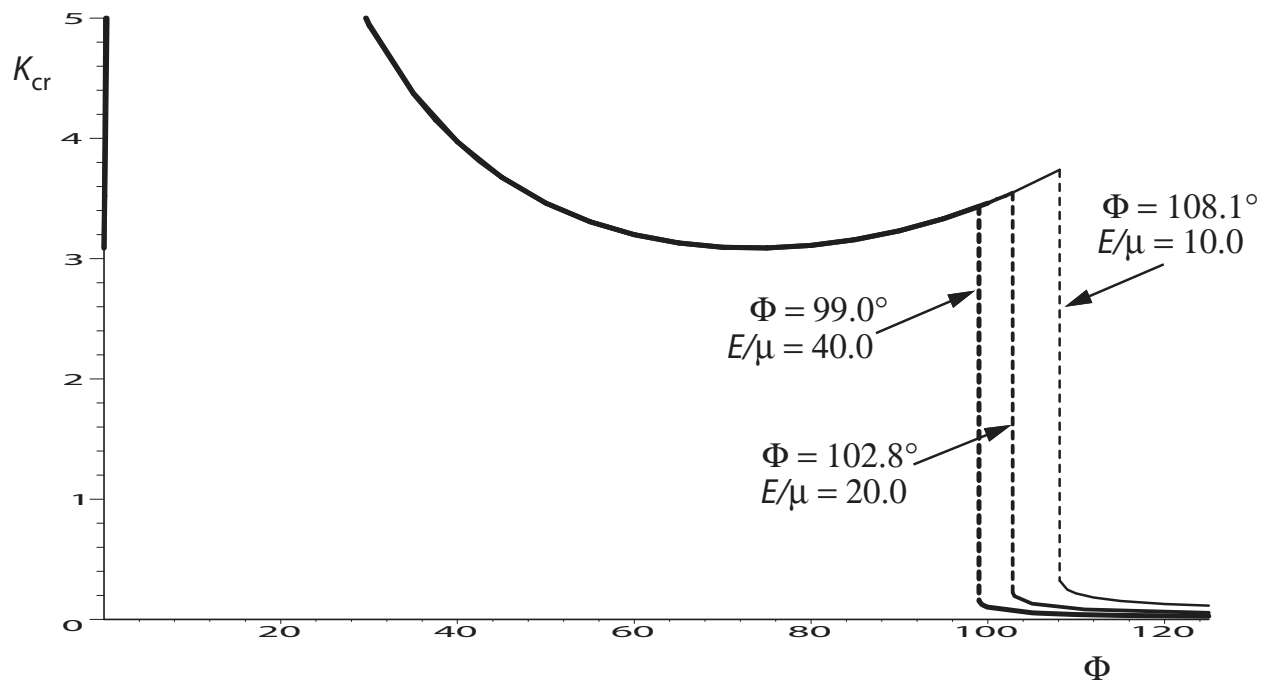


Fig. 5 Variations in the critical amount of shear for surface instability with the angle between the directions of shear and the fibers. The solid is modeled as a neo-Hookean matrix reinforced with one family of fibers (standard reinforcing model); the ratio of the matrix shear modulus to the fiber stiffness is taken in turn as 40.0, 20.0, and 10.0. The three graphs coincide as long as $0 < \Phi < \Phi_0$, where $\Phi_0 = 99.0$ deg, 102.8 deg, and 108.1 deg, respectively. At $\Phi = \Phi_0$, the half-space switches from being very stable ($K_{cr} > 3.09$) to being easily unstable ($K_{cr} < 0.3$). The part of the plot corresponding to $K_{cr} > 5$ is not shown for physical and visual reasons.

order to double check our numerical computations.

The crucial boundary condition is to find the amount of shear at which the surface of the sheared solid is free of tractions. The safest way to express this is

$$\det \mathbf{Z} = 0 \quad (27)$$

where \mathbf{Z} is the (Hermitian) *surface impedance matrix*, which relates tractions to displacements through $\mathbf{S} = i\mathbf{Z}\mathbf{U}$. We remark that the schemes are not as safe in surface stability problems as they are in the surface wave theory because of incompressibility [13,14] and nonmonotonicity of $\det \mathbf{Z}$ with K .

Once Eq. (27) is reached, we can construct an incremental solution to the equations of equilibrium, which is adjacent to the large shear equilibrium and signals the onset of surface instability. We adopted the following strategy:

- (i) Fix Φ , the angle between the direction of shear and the preferred direction.
- (ii) Fix θ , the angle between the direction of shear and the normal to the wrinkles' front.
- (iii) Find (if it exists) the corresponding critical amount of shear such that Eq. (27) is satisfied.

Then repeat steps (ii) and (iii) for other angles θ until the entire surface is spanned, and keep the smallest critical amount of shear K_{cr} (say) for the angle Φ chosen in step (i). Then take a different value of Φ until all possible fiber orientations are covered. In fine a graph of K_{cr} as a function of Φ is generated.

5 Numerical Results for Biological Soft Tissues

We take the *standard reinforcing model*,

$$W = \mu(I_1 - 3)/2 + E(I_4 - 1)^2/4 \quad (28)$$

where E is an extensional modulus in the fiber direction. This model has been used for several soft tissues, such as papillary

muscle [19], myocardium [19], skeletal muscles [20], or brainstem [21].

That latter reference examines the ability of the constitutive model (Eq. (28)) to describe the mechanical response of porcine brainstem specimens. Recall that large deformations, particularly large shears, of brain tissues are often associated with traumatic brain injuries (Doorly and Gilchrist [22]). Ning et al. [21] found that the model provides good agreement with experimental data; they estimate that for 4 week old pigs, E is about 20 times larger than μ . In a recent review on physical properties of tissues for arterial ultrasound, Hoskins [23] emphasized the need for constitutive models of a nonlinear elastic behavior. He also collects available data for arterial walls: in particular, for abdominal aortic aneurysms, ex vivo measurements indicate that E is about 10 times larger than μ , while for human atherosclerotic plaque, E seems to be more than 40 times μ . For our numerical computations, we take in turn the values $E/\mu = 40.0$, 20.0 , and 10.0 and collect the corresponding results in Fig. 5.

Broadly speaking, we find a region where the solid is strongly reinforced by the family of fibers, followed by an abrupt drop in the value of the critical amount of shear for surface instability, which occurs earlier as E/μ increases.

When the fibers are aligned with the direction of shear, they are not stretched and they play no role; thus it is appropriate that at $\Phi = 0.0$ deg, we find $K_{cr} = 3.09$, the critical amount of shear for an isotropic neo-Hookean half-space (see Sec. 2).

Next we find that K_{cr} shoots up to unrealistic values when $\Phi \geq 0.0$ deg: for instance, $K_{cr} = 32.48$ when $\Phi = 3.0$ deg (not represented for visual convenience). Hence, the solid is strongly reinforced with respect to surface stability when the shear takes place more or less along the fibers: wrinkling is prevented.

As the angle Φ between the shear and the fibers increases, the critical amount of shear goes through a maximum, then a minimum, always remaining above 3.09, the value for an isotropic neo-Hookean half-space, as long as $\Phi \leq \Phi_0$, where $\Phi_0 = 99.0$ deg,

102.8 deg, 108.1 deg, approximately, for $E/\mu=40.0$, 20.0, and 10.0, respectively. It is worth noting that in the range $90.0 \text{ deg} < \Phi < \Phi_0$, the fibers undergo a slight compression at low shear levels and are then in extension until the critical amount of shear is reached; even when the fibers are compressed, the half-space remains stable.

When the angle Φ is large, $\Phi_0 < \Phi < 180.0 \text{ deg}$, the half-space becomes unstable at low amounts of shear. For instance, at $\Phi = 99.07 \text{ deg}$, we find that $K_{cr}=0.153$ when $E/\mu=40.0$; note that in reaching that critical amount of shear, the fibers are compressed by less than 1.3%. The switch from high to low critical amounts of shear is abrupt due to the nonmonotonicity of $\det \mathbf{Z}$ with K : this quantity has a minimum in the high range ($K > 3.09$), which is always negative (indicating the existence of a root to Eq. (27)), but it can also have a minimum in the low range ($K < 0.3$). This minimum is positive when $\Phi < \Phi_0$ (no root in Eq. (27)) but negative when $\Phi > \Phi_0$, hence the jump in K_{cr} .

Finally we note that in the range $\Phi_0 < \Phi < 180.0 \text{ deg}$, the angle θ normal to the wrinkles' front is close to Φ (within 2 deg), indicating that the wrinkles are almost at right angle with the fibers; these predictions are in accordance with the observation of Fig. 1.

6 Discussion

We developed a quantitative methodology to understand the formation of wrinkles in some biological soft tissues. The analysis allowed us to model some visual observations of a sheared elastomer versus a sheared piece of skeletal muscle based on a simple nonlinear anisotropic constitutive law (requiring the knowledge of only one quantity, E/μ).

Studying the geometry and mechanics of wrinkles is relevant to many biomechanical applications such as the treatment of scars, and our results may provide some help in developing rational approaches to these problems. The next logical step is to apply and generalize this methodology to model the wrinkling of skin and other biological membranes. These may require more work than presented here, with the consideration of two families of parallel fibers (the collagen network), but the methodology remains essentially the same. It is also exact, versatile, and more convenient to apply than methods based on approximate theories (e.g., Föppl-von Kármán plate equations) because it can easily accommodate anisotropy, nonlinear constitutive laws, finite thickness, and large homogeneous predeformation.

Acknowledgment

We thank the Centre National de la Recherche Scientifique, the Irish Research Council for Science, Engineering and Technology,

Enterprise Ireland, and the City of Paris for their support through international collaboration grants.

References

- [1] Biot, M. A., 1963, "Surface Instability of Rubber in Compression," *Appl. Sci. Res., Sect. A*, **12**, pp. 168–182.
- [2] Ogden, R. W., 1984, *Non-Linear Elastic Deformations*, Ellis Horwood, Chichester.
- [3] Green, A. E., and Zerna, W., 1954, *Theoretical Elasticity*, Oxford University Press, Oxford.
- [4] Flavin, J. N., 1963, "Surface Waves in Pre-Stressed Mooney Material," *Q. J. Mech. Appl. Math.*, **16**, pp. 441–449.
- [5] Spencer, A. J. M., 1984, *Continuum Theory of the Mechanics of Fiber Reinforced Composites*, CISM No. 282, Springer, New York.
- [6] Ogden, R. W., 2003, *Non-Linear Elasticity With Application to Material Modelling*, Institute of Fundamental Technological Research, Warsaw.
- [7] Chadwick, P., and Whitworth, A. M., 1986, "Exceptional Waves in a Constrained Elastic Body," *Q. J. Mech. Appl. Math.*, **39**, pp. 309–325.
- [8] Prikazchikov, D. A., and Rogerson, G. A., 2004, "On Surface Wave Propagation in Incompressible, Transversely Isotropic, Pre-Stressed Elastic Half-Spaces," *Int. J. Eng. Sci.*, **42**, pp. 967–986.
- [9] Merodio, J., and Ogden, R. W., 2002, "Material Instabilities in Fiber-Reinforced Nonlinearly Elastic Solids Under Plane Deformation," *Arch. Mech.*, **54**, pp. 525–552.
- [10] Chadwick, P., 1997, "The Application of the Stroh Formalism to Pre-Stressed Elastic Media," *Math. Mech. Solids*, **97**, pp. 379–403.
- [11] Destrade, M., and Ogden, R. W., 2005, "Surface Waves in a Stretched and Sheared Incompressible Elastic Material," *Int. J. Non-Linear Mech.*, **40**, pp. 241–253.
- [12] Destrade, M., Otténio, M., Pichugin, A. V., and Rogerson, G. A., 2005, "Non-Principal Surface Waves in Deformed Incompressible Materials," *Int. J. Eng. Sci.*, **43**, pp. 1092–1106.
- [13] Fu, Y. B., 2005, "An Explicit Expression for the Surface-Impedance Matrix of a Generally Anisotropic Incompressible Elastic Material in a State of Plane Strain," *Int. J. Non-Linear Mech.*, **40**, pp. 229–239.
- [14] Fu, Y. B., 2005, "An Integral Representation of the Surface-Impedance Tensor for Incompressible Elastic Materials," *J. Elast.*, **81**, pp. 75–90.
- [15] Triantafyllidis, N., and Abeyaratne, R., 1983, "Instabilities of a Finitely Deformed Fiber-Reinforced Elastic Material," *ASME J. Appl. Mech.*, **50**, pp. 149–156.
- [16] Qiu, G. Y., and Pence, T. J., 1997, "Loss of Ellipticity in Plane Deformation of a Simple Directionally Reinforced Incompressible Nonlinearly Elastic Solid," *J. Elast.*, **49**, pp. 31–63.
- [17] Farnell, G. W., 1970, "Properties of Elastic Surface Waves," *Physical Acoustics* Volume 6, W. P. Mason and R. N. Thurston, eds., Academic, New York, pp. 109–166.
- [18] Destrade, M., 2005, "On Interface Waves in Misoriented Pre-Stressed Incompressible Elastic Solids," *IMA J. Appl. Math.*, **70**, pp. 3–14.
- [19] Taber, L. A., 2004, *Nonlinear Theory of Elasticity*, World Scientific, NJ.
- [20] Röhrle, O., and Pullan, A. J., 2007, "Three-Dimensional Finite Element Modelling of Muscle Forces During Mastication," *J. Biomech.*, **40**, pp. 3363–3372.
- [21] Ning, X., Zhu, Q., Lanir, Y., and Margulies, S. S., 2006, "A Transversely Isotropic Viscoelastic Constitutive Equation for Brainstem Undergoing Finite Deformation," *ASME J. Biomech. Eng.*, **128**, pp. 925–933.
- [22] Doorly, M. C., and Gilchrist, M. D., 2006, "The Analysis of Traumatic Brain Injury Due to Head Impacts Arising From Falls Using Accident Reconstruction," *Comput. Methods Biomech. Biomed. Eng.*, **9**, pp. 371–377.
- [23] Hoskins, P. R., 2007, "Physical Properties of Tissues Relevant to Arterial Ultrasound Imaging and Blood Velocity Measurement," *Ultrasound Med. Biol.*, **33**, pp. 1527–1539.